Volume 16, Number 1, 2023. pp. 105-118

Jordan Journal of Physics

ARTICLE

Morphological Design of the Photonic Crystals Influence on Improving the Optoelectronic Properties of a-SiGe:H Thin Film Solar Cell

Boumediene Sadoun[a], **Souheil Mouetsi**[a], **Abdesselam Hocini**[b] and **Roumaissa Derdour**[a]

[a] *Laboratory of Electronics and New Technology (LENT), Department of Electrical Engineering, Faculty of Sciences and Applied Sciences, University of Oum el bouaghi, Ain beida, 04201, Algeria.*

[b] *Laboratory of Signal and Systems Analysis (LSSA), Department of Electronics, Faculty of Technology, University of M'sila, 28000, Algeria.*

Doi: **https://doi.org/10.47011/16.1.11**

Received on: 20/06/2021; *Accepted on: 02/08/2021*

Abstract: With their nano-engineered feature, Photonic Crystals (PhCs) allow the best control of the propagation and absorption of light in an increased way. In our work, we applied the Rigorous Coupled Wave Analysis (RCWA) method to calculate the diffraction efficiency, field distribution, for a specific incidence angle and absorption energy in a periodic structures using unpatterned, 1DPhC, half circle and triangular grating structures with both a-Si:H, a-SiGe:H thin film semiconductor materials with different gratings of PhCs to improve optical absorption, taking into account the J-V solar cell characteristics. According to our simulation, the ideal result was in the case of triangular grating with a-SiGe:H semiconductor material so for the presence of Germanium, which enhances light absorption by reducing the band gap energy. The optical light absorption was more than 85.7% by increase the lattice parameter from 0.3µm to 0.5µm. Moreover, we found a solar cell efficiency enhancement of 16.6%, with a total improvement of 7.74%; as compared with unpatterned grating. Concerning the incidence angle effect, the better one is ranged between 50° and 70° with a peak absorption ratio of 99%.

Keywords: Photonic crystals, RCWA, Incidence angle, Triangular grating, Solar cell.

Introduction

Photovoltaic (PV) is one of the energies that can provide an answer to the current energy problem. Although it represents a very small part of the world's energy production, it has increased by more than 45% per year in the past [1]. Most industrial solar cells are fabricated using polycrystalline or mono-crystalline silicon. However, the main disadvantages of this type of production are the high cost of the material and the high-energy consumption during production. The production of PV energy comes from the principle of the photoelectric effect which corresponds to the phenomenon of the transformation of light energy into electrical energy. Enhancing and optimizing the effect of PV characteristics, depends on the quality of the used semiconducting materials. This should be taken into consideration, as it's directly concerning the cell's execution. Manufacturing PV cells has evolved over several generations, as shown in Fig. 1, where in our work, we relied on the second generation thin film of solar cells.

Corresponding Author: Boumediene Sadoun **Email**: sadoun.boumediene@univ-oeb.dz

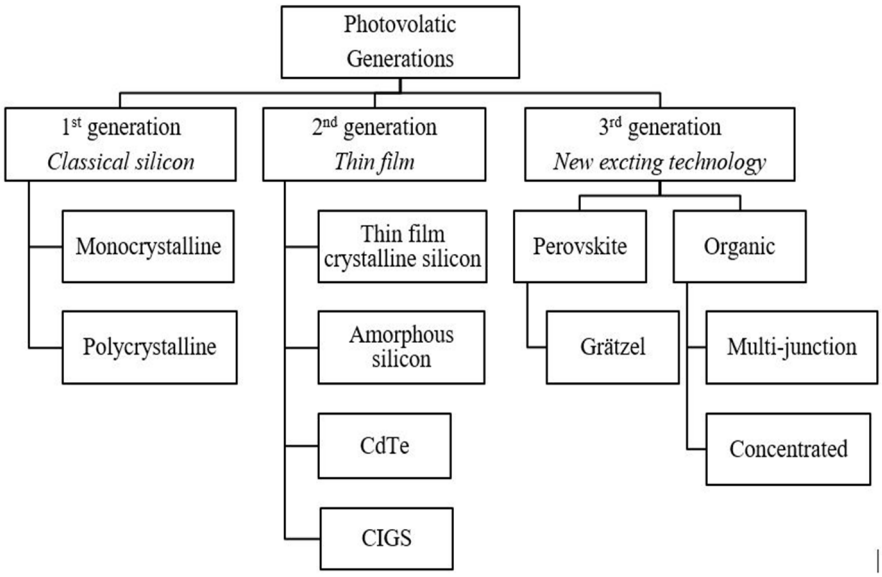

FIG. 1. Development stages of PV cell generations [2].

Among the methods used to enhance the light absorption in solar cells, the Anti-Reflection Coatings (ARCs) and the surface texture [3]. Moreover, Photonic Crystals (PhCs) is also a method, in which recent studies have shown its efficiency to enhance photon beams flow absorption, the main advantage of PhCs is in the light control of wavelength [4]. PhCs are periodic structures of dielectric or metallo-dielectric materials, whose permittivity is adjusted periodically in one, two or three dimensions in space, which makes it possible to create a photonic band gap in order to enclose the light so it cannot spread [5]. Semiconductor materials have an electrical conductivity which can be controlled by doping process or photon beams, it can be distributed according to their chemical composition like Silicon (Si) or molecular structure like organic semiconductors [6].

Most of the commercial PV technology used depends on the crystalline silicon that has useful properties and low cost, many efforts in recent years have been devoted to the development of thin film of solar cell prototype [7]. In 2016, Smith, D *et al*. found the silicon cell efficiency η equal to 25.2% [8], one year later, Yoshikawa, K *et al*. [9], found it increased relatively to 26%. Furthermore in 2020, Green, M. A *et al.* found an increase in the silicon efficiency of the silicon solar cell that is up to 26.7% [10]. The efficiency of solar cells remains low, because the purity of the material is lower, and the effective area is reduced. This is affected by the flow of sunlight and avoiding shaded places. It is also to prevent the increase in temperature and to maintain their stability. In addition, a lot of energy is lost due to thermal effects [11]. The optical absorption of the solar cells depends on the active material, which motivated us to employ PhCs to improve the absorption based on crystals pertinent properties [12].

Our contribution consists of enhancing the absorption ratio of the photon beams in by the active thin film of the solar cells by employing the PhCs technology. Therefore, we investigated the ability of absorbing photon beams in the visible light spectrum by active PV thin film of 0.1μm thickness [13], based on the morphological effect of different structures for One-Dimensional Photonic Crystal (1DPhC). Thus, we have studied the optical and the electrical properties of two types of semiconductor materials (a-Si:H and a-SiGe:H). The a-Si:H, is more sensitive and responsive to solar radiation due to the presence of hydrogen atom H_2 [14]. On the other hand, the presence of germanium in a-SiGe:H enhances the light absorption by reducing the band gap energy [15].

The simulation approaches in this work were performed on the RCWA method using RSoft CAD layout software that relies on the Maxwell equations to improve and analyze the effectiveness of thin film solar cell structures [16].

The Used Semiconductor Materials

Most of the solar cells are made of silicon since it is readily available and is inexpensive. The major drawback of using germanium is the

effect of the temperature which affects stability. On the other hand, its most important advantage is its conductivity, which is higher than the silicon's, in addition to the process of absorption which is also at a significant pace. This will certainly facilitate the stability of solar cells [17].

The a-Si:H is characterized by the presence of a hydrogen atom (H_2) which allows the solar cell to be more sensitive to photon beams to enable it to have higher absorption [18]. Amorphous films characteristics should be improved to attain the prime performance of a-Si:H thin film which requires sophisticated devices and materials. a-SiGe:H thin film is famed to be one of the favorable PV devices and it is prepared from a blend gas of GeH_4, H_2 and SiH_4, which is fabricated with several deposition techniques, usually, with Plasma Enhanced Chemical Vapor Deposition (PECVD) or Hotwire Chemical Vapor Deposition (HWCVD) [19]. The properties of a-SiGe:H depend on both Germanium [Ge] and Hydrogen [H] contents. The hydrogen in a-SiGe:H content given by:

$$[H] = \frac{[H_2]}{[Si+Ge]} \quad (1)$$

The germanium content formulated by:

$$[Ge] = \frac{[G_e]}{[Si+Ge]} \quad (2)$$

Generally, both Rutherford spectroscopy for background dispersion and X-ray spectroscopy methods can determine germanium concentration. The Germanium material content variation in a-SiGe:H contributed to reducing the optical band gap, which can be the most important characteristic of the latter as compared with a-Si:H [15]. The a-SiGe:H and hydrogenated a-Si, is an already commercialized solar cell as compared to thin film amorphous silicon. Amorphous silicon cannot be manufactured by rapidly cooling the melting silicon, instead the amorphous material is prepared by sedimentation from the gas phase on substrates that are kept at temperatures well below the melting temperature [20]. Thereupon, the advantage of using a-SiGe:H is the smaller energy gap and, hence, it can collect more radiation and increase the photo-conversion solar cell efficiency [21].

Table 1 shows the physical parameters of a-SiGe:H and a-Si:H, in which the thin film of the solar cell was made.

TABLE 1. The physical parameters of a-Si:H and a-SiGe:H thin films [22].

The physical parameters	a-Si:H	a-SiGe:H
Band gab [eV]	1.7 -1.8	1.0 -1.7
DC dielectric [$F.m^{-1}$]	3.9	3.75
Permittivity [$F.m^{-1}$]	20.1306	24.6613
Electron affinity [eV]	1.75	1.39
Photo-conductivity [s/cm]	10^{-4}-10^{-5}	10^{-5}-10^{-7}
Urbach energy [meV]	42-50	>45
Thermal-conductivity [$W.m^{-1}.K^{-1}$]	1.38	1.36
Light-induced decomposition after 1000 hours [%]	15-30	10-20

Simulation Modeling and Analysis Method

There are various methods of numerical modeling that can be used to analyze the diffraction of electromagnetic waves on periodic gratings. Among these methods, we used the Rigorous Coupled Wave Analysis method (RCWA) implemented in the RSoft layout software [23]. The RCWA method is integrated in the RSoft CAD layout software to perfectly and precisely generate both periodic and non-periodic components without piecewise approximation assumptions. It epitomizes the electro-magnetic domains as the sum of all paired waves and a periodic permittivity function which is embodied using Fourier harmonics. Allowing the full vectorial Maxwell equations to be solved in the Fourier field, thus the diffraction efficiencies are computed at the end of the simulation, and the spatial fields distributions are derived from the Fourier harmonics [24]. It is applicable to sub wavelength structures and PhCs.

Moreover, the RCWA functions as a template for producing computational programs; thus, affording a more systematic procedure to deal with complex geometries, particularly those comprising beneficial electric conductors. The latter solves full vectorial types of Maxwell's equations, and deals with a wide range of scattering complications on structures with

horizontally periodic boundary conditions. Arbitrarily vertical variations can be handled, however the cover and substrate must be homogenous [25].

In our work, we applied the RCWA method to calculate the diffraction efficiency, field distribution, for a specific incidence angle and absorption energy in a periodic structures using unpatterned, 1DPhC, half circle and triangular grating structures with both a-Si:H, a-SiGe:H thin film semiconductor materials. On the other hand, we studies the electrical properties of the forgoing grating structures with a-Si:H and a-SiGe:H in order to compute the total maximum power, filling factor, open circuit voltage, short circuit current density, reverse bias saturation current and the solar cell efficiency.

Results and Discussions

A numerical simulation has been placed to enhance the dimensions of the diverse types of PhCs. Table 2 shows the values of the optical properties calculated by employing the RSoft CAD layout software, which we were able to model an integrated solar cell thin film with unpatterned and 1DPhC by using the two semiconductor materials a-Si:H and a-SiGe:H in the linear regime.

TABLE 2. The used parameters of a-Si:H well as a-SiGe:H for thin film PV cells with PhCs used in the linear regime.

Parameters	The value
Free space wavelength [µm]	0.63
Lattice cte (period) [µm]	0.5
k_0 [m^{-1}/s^{-1}]	(2. π)/free space wavelength
Wavelength corresponding to the band gap (λg) [µm]	1.107
Frequency [HZ]	1/free space wavelength
Substrate of glass (refractive index)	1.5
Total hydrogen concentration [cm^{-3}]	5.0 x10^{21}
Total electron concentration [cm^{-3}]	2.0 x10^{23}
Defect state density freeze in temperature [K]	500

Optical Properties

Absorption in Unpatterned and 1DPhC Gratings

The subsequent step in the manufacturing process depends on the immediate conveyance of PhCs from the unpatterned absorbent layer to the patterned layer. Fig. 1.a and Fig. 1.b below present the active layer infrastructure in linear regime, the Fig. 2.a show an unpatterned absorbent thin film on a substrate of glass, whereas, the second consists of a 1DPhC absorbent thin film on a glass substrate. Two types of grating structures are made by a-Si:H and a-SiGe:H semiconductor materials.

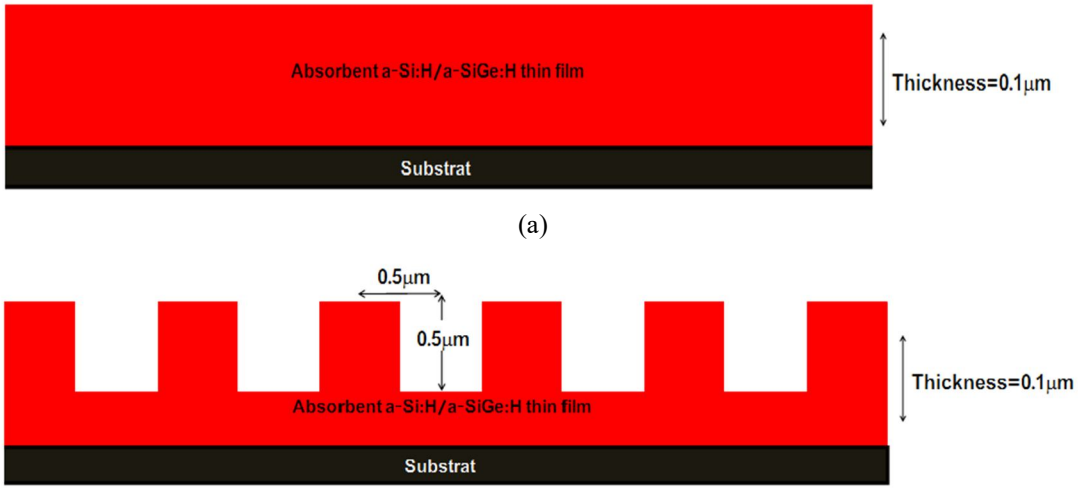

FIG. 2. (a) Unpatterned and (b) 1DPhC lattice structures, made by a-Si:H and a-SiGe:H respectively.

The emitted light resonance depends on the associated wavelength with the same parameters of two grating structures. In both unpatterned and 1DPhC, the specific parameters are wavelength (λ), the lattice parameter constant (L = 0.5µm), the layer's width (D) likewise equal to 0.5µm. The thicknesses of two arrangement grating structures are considered the same, they are equal to 0.1µm.

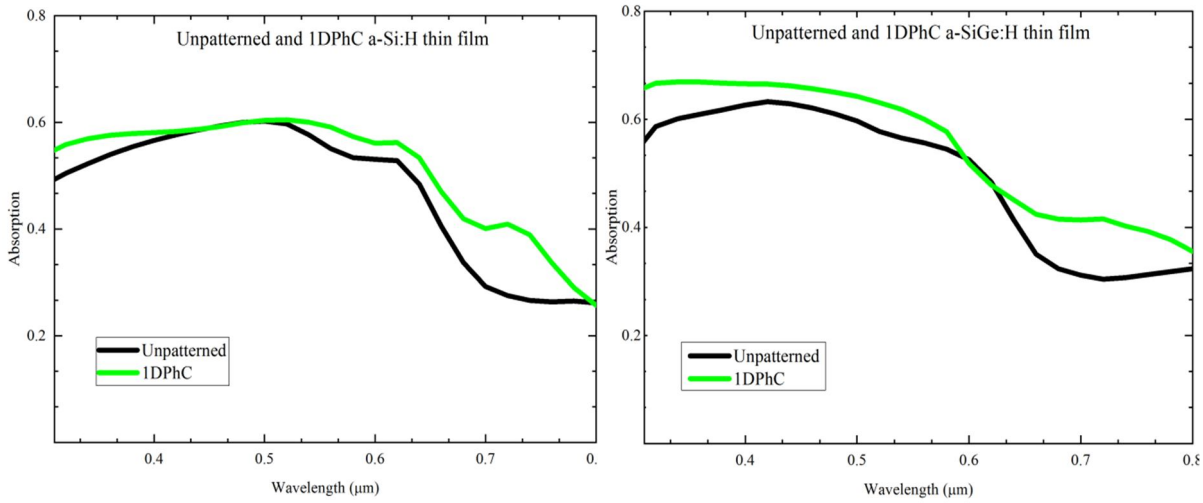

(a) (b)

FIG. 3. Optical absorption of (a) a-Si:H thin film made by unpatterned and 1DPhC, (b) a-SiGe:H thin film made by unpatterned and 1DPhC lattice structures.

In Fig. 3.a and Fig. 3.b we gave the absorption energy of the a-Si:H and a-SiGe:H. For TE-polarized light, absorption control was at different wavelength points of the visible light spectrum. We notice that the spectra corresponding to the layers of a-SiGe:H are different from the spectrum of the a-Si:H thin layers as below. For the a-Si:H semiconductor material, the 1DPhC is more adequate than unpatterned lattice structure; where the highest absorption ratio is 63.37% when the lattice constant was between (0.462µm to 0.546µm) and reached to 58% in unpatterned one, then it begins to decrease due to the extinction coefficient (*k*) in both structures until the ratio reaches 25.99% at lattice constant of 0.8µm. The absorption ration was up to 62.9% for unpatterned and reaches to 68.7% once the pattern period was between 0.398µm and 0.455µm with a-SiGe:H semiconductor material in 1DPhC. This absorption ration was greater than of a-Si:H. Furthermore, the absorption ratio was decreasing to reach 35.5% in 1DPhC at grating period of 0.8µm and up to about 30.4% in the unpatterned lattice. Correspondingly, the enhancement of the absorption ratio in the lattice constant between 0.3µm and 0.5µm in 1DPhC of two types of materials is around 5.8%. Additionally, the absorption in the solar cells is affected by the presence of proportion germanium in a-SiGe:H compared to the a-Si:H used in the manufacture of the thin film solar cell, as well as PhCs which can increase the absorption rate.

Ouanoughi, A *et al*. [26], conducted a numerical simulation to design the geometry of a solar cell made by 1DPhC in order to improve its absorption. Their results show an enhanced absorption in 1DPhC grating structure that is apparent compared to the unpatterned one, which proves the ability of the structure to produce PhCs solar cells. In addition to this, for wavelengths range of lattice constant of 0.38µm and 0.5µm, we found an enhancement in the absorption ratio with 24% in unpatterned and 3.37% in 1DPhC grating with a-Si:H thin film, whereas in the case of the a-SiGe:H thin film, the enhancement in the absorption ratio was 28% which higher than in a-Si:H with unpatterned and 8.7% with 1DPhC lattice.

This enhancement due to employing grating period pattern is due to the light trapping effect which is mainly attributed to Fabry–Pérot resonance modes due to the large index contrast between air and semiconductor layer, which is ubiquitous in the thin film layer, where it can excited by the micro cavity resonance influence, which can trap light effectively [27].

Optimal Morphological Design

In this part, we exploit the effect of the morphology of the structure of the absorbing layers on the absorption rate. For this reason, we studied various grating structures (half circle and triangle).based on previous studies [28].

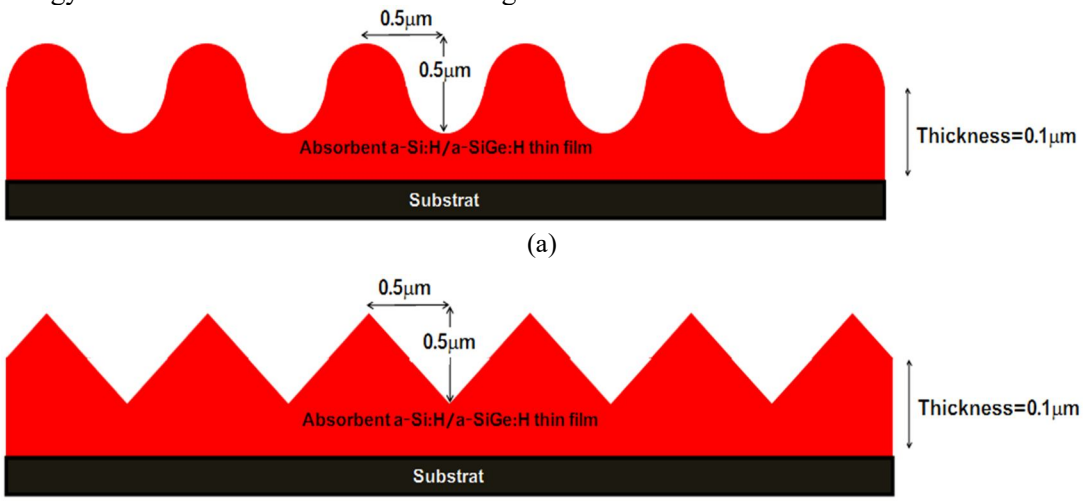

FIG. 4. Geometrical grating of (a) half circle, (b) triangle gratings made by a-Si:H and a-SiGe:H.

Fig. 4 (a and b) represents the studied grating structures of the half circle and the triangle, based on both a-Si:H and a-SiGe:H semiconductor materials with the same lattice constant (0.5µm), the same thickness (0.1µm) and the same visible light in the optical wavelength for TE-polarized of the light deposited on a glass substrate. In this case we preserve the used parameters in Table 2. For the proposed two structures, a half circle that can be used to construct arithmetic and geometric means of lengths, we use a radius of 0.25µm. On the other hand, we use the isometric triangle where all the three sides are of the same length, all the three angles are equal to 60°, with a height and width equal to 0.5µm. Fig. 5 shows the geometrical dimensions of both shapes.

FIG. 5. Dimensions of the simple proposed gratings of (a) half circle and (b) isometric triangle.

Both structures were extracted from the RSoft CAD premium numerical simulation software and integrated with the RCWA method which is based on the diffracted diffusion of light waves.

Fig. 6 represents the simulation results of the absorption energy of both a-Si:H and a-SiGe:H semiconductor material with half circle and triangular gratings.

In Fig. 6.a, the absorption in triangle grating reaches 69.7%, however it is equal to 65.6% in half circle grating during (~0.3µm-0.5µm). After that, the absorption ratio was decreasing under the influence of extinction coefficient (k) until lattice parameter is equal to 0.8µm, which achieves 26% for triangle and 24.7% in half circle gratings. In Fig. 6.b in comparison with a-Si:H, a noticeable improvement of peak absorption energy with a-SiGe:H which is estimated at 16% an enhancement of the absorption in the triangular structure which is 5.4% in the half circle grating in the range from 0.3µm and 0.5µm (the best visual field absorption). PhCs dimensions have been improved by integrated design of numerical simulation and experiment techniques. While we use different grating structures for 1DPhC based on a-Si:H and a-SiGe:H, we found that the

absorption ratio in triangular grating is better compared to the half-circle grating. The obtained results are in good agreement with previously reported by Dominguez, S *et al.* [29] and Heidarzadeh, H with Tavousi, A [30], who showed that the triangular structure is better grating for the optical absorption enhancement, which allowed more photon beams to come into thin film of PV cell to enhance the absorption efficiency by using the dispersion influence.

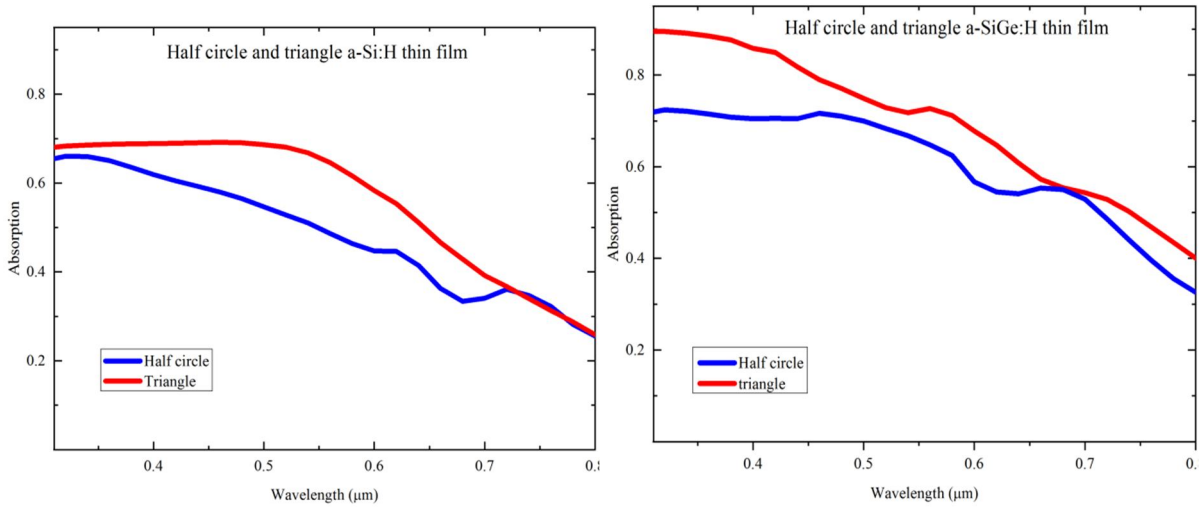

(a) (b)

FIG. 6. Optical absorption of the half circle and triangle gratings made by (a) a-Si:H and (b) a-SiGe:H.

The geometrical parameters have an important effect on the distribution spectral of the absorbent PhCs, which can be done in the full distance of wavelength if the PhCs dimensions are adequately altered. However, the obstacles and reasons that are still being studied currently about the efficiency and absorption capacity of solar cells is silicon PV processing that is still very expensive. Its low efficiency is also due to some properties including the crystal structure, the membrane quality, the conductive layers and the interfaces as well as alternative designs and anti-reflective coatings [31].

The light absorbs from the absorber layer of the PV cell. Additionally, when the absorption is from all layers of the solar cell, there is a loss and an efficiency decrease, this is named parasitic absorption [32]. While for triangle lattice, the waveguide mode resonance or leaky mode resonance effects lead to light trapping and increase the absorption in the active layer. In addition, the morphological effect on photonic crystals with different dimensions can excite micro cavity resonance effects, which can trap light effectively [33].

Both the excellent geometrical properties and micro cavity effect make the triangle grating outperform the 1DPhC and half circle grating structures.

Electronic Properties

The solar cell is distinguished under the AM1.5G insulation by means of current density versus voltage J-V with the characteristic device parameters (V_{oc}, J_{sc}, *ff*, η) and external quantum efficiency (EQE) properties. In this section the electrical properties of each grating used with two types of semiconductor materials (a-Si:H and a-SiGe:H) are investigated based on several electrical output parameters;

V_{oc}[V] is the open circuit voltage where no current flows through the external circuit [34]. It is the maximum voltage that a solar cell can be delivered in. It is done by:

$$V_{oc} = \frac{kT}{q} \ln\left(\frac{J_{sc}}{J_{so}} + 1\right) \quad (3)$$

where: k[J.K^{-1}] is Boltzmann's constant; T[K] the absolute temperature; q[eV] the electron energy; J_{so}[mA/cm^2] the reverse bias saturation current; J_{sc}[A/cm^2] the short circuit current density [35]. Where η[%] is the ratio of energy output from the solar cell to the input energy from the sun, given by:

$$\eta = \frac{P_{max}}{P_{in}} = \frac{J_m \times V_m}{P_{in}} = \frac{J_{sc} \times V_{oc} \times ff}{P_{in}} \quad (4)$$

with: P_{max}[W] is the total maximum power; P_{in}[W/m^2] is the total incident power; *ff* is the filling factor; it can be defined as the ratio of the actual maximum obtainable power to the product

of the open circuit voltage and short circuit current, we obtained it from the device J-V curve or using the following equation [36]:

$$ff = \frac{J_m \times V_m}{J_{sc} \times V_{oc}} \quad (5)$$

where: J_m[A/cm^2] is the maximum current density; V_m[V] is the maximum voltage. In this section, we studied different shapes of 1DPhC with a-Si:H as absorber thin film, by using the RCWA method. Fig. 7 shows the simulation results of a thin film PV cell made by a-Si:H, depending on grating morphology of structures, respectively under AM1.5G insulation.

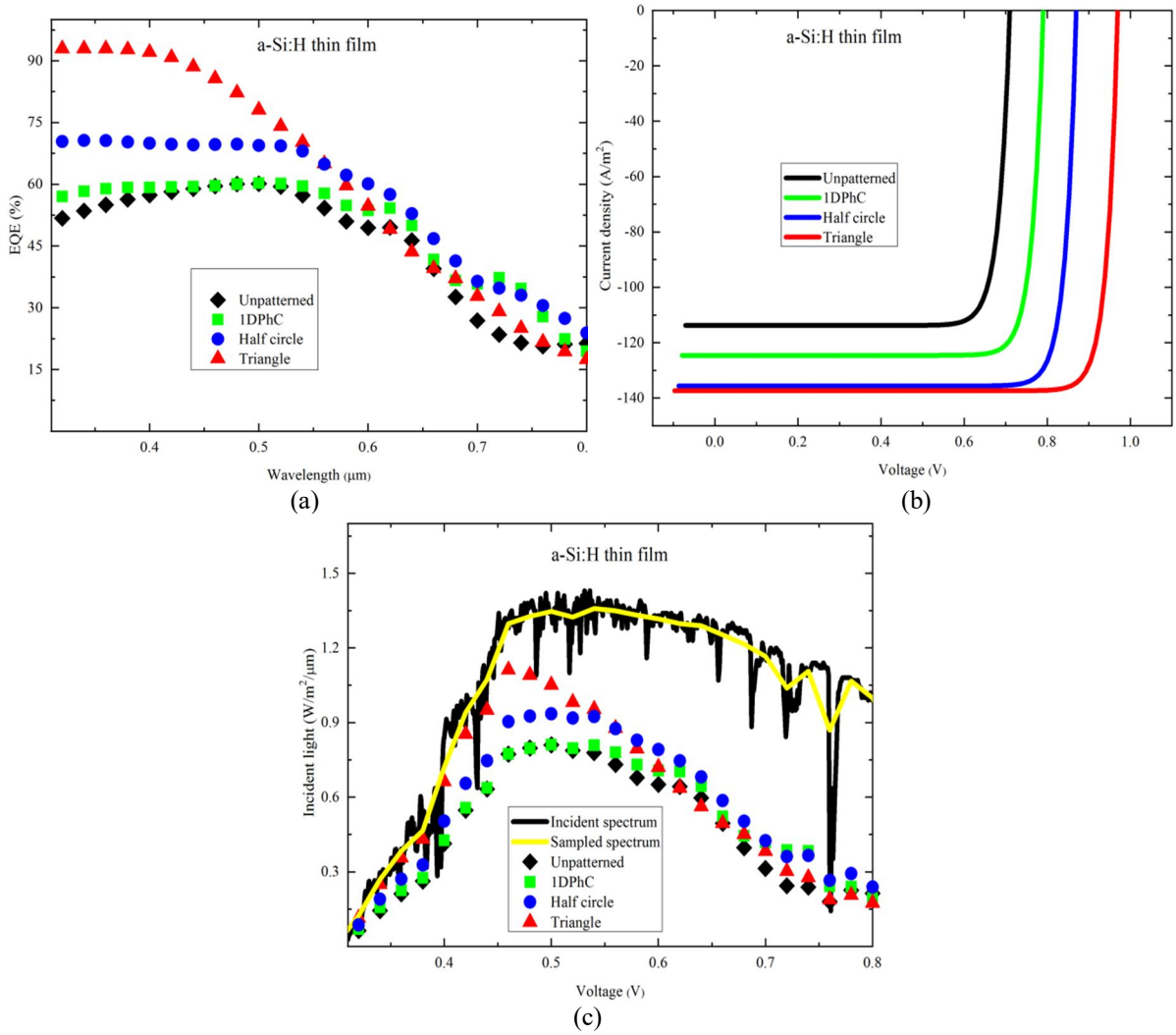

FIG. 7. (a) the EQE graphs, (b) the J-V curves and (c) smooth spectral distribution of the studied AM1.5 solar spectrum with different grating structures studied made by a-Si:H of thin film solar cells.

Fig. 7.a shows the EQE curves of a-Si:H thin film solar cells with varying PhCs shapes using improved geometrical parameters. Correspondingly, Fig. 7.b shows J-V curves of a a-Si:H thin film solar cell leading to outstanding values of V_{oc} and J_{sc} and Fig. 7.c shows the computed spectral distribution graph for the proposed simple gratings for the studied solar spectrum AM1.5. The net current is always flowing from one contact towards the other, where it is always positive relative to one contact and negative relative to the other. Thus, the direction of the current measured only depends on which electrode you reference to ground and the measured current sign does not depend on or affect the physics charge within the device [35]. We can summarize the results in the following table:

TABLE 3. The simulation results of a-Si:H thin film solar cell energy conversion efficiency.

	Unpatterned	1DPhC	Half-circle	Triangular
P_{max}[W]	68.4	84.57	102.59	117.20
ff [%]	84.75	85.92	86.9	87.94
V_{oc}[V]	0.71	0.79	0.87	0.97
J_{sc}[A/cm^2]	113.8	124.6	135.7	137.4
J_{so}[A/cm^2]	109.3	120.2	131.3	133.4
η[%]	7.61	9.4	11.4	13.01

The better result in the a-Si:H case, was the triangle grating with the highest values of all electrical parameters of efficiency. The efficiency was found to reach 13.01%, the total improvement efficiency among the unpatterned and triangle models was 5.4%. However, the maximum power noticed in the triangle model is 117.20W, which makes a difference of 48.8W over the unpatterned grating structure. The results showed that the cell efficiency with a-Si:H, presents useful numerical simulation results. This makes the doping semiconductor materials suitable in terms of absorption efficiency, as well as being more sensitive to the sunlight. As clearly seen in Fig. 7 and Table 3, we can explain the reason for the increase in the J-V characteristics devises parameters, where V_{oc}, *ff* and the efficiency of different grating structures is progressively higher in order to reduce the recombination loss affecting V_{oc}, the parasitic resistance losses which primarily limit the *ff* as well as V_{oc} and J_{sc}, and eventually optical losses which have a large effect on photo-generated carriers and J_{sc}. The EQE values shown in Fig. 7.a, where the highest value was at triangle case in the point 0.3µm of the wavelength, where it makes a difference of 0.41V than unpatterned one.

Additionally, Fig. 8 presents the numerical simulation of the a-SiGe:H thin film PV cell lattices on linear regime with the same parameters as above, under the AM1.5G insulation.

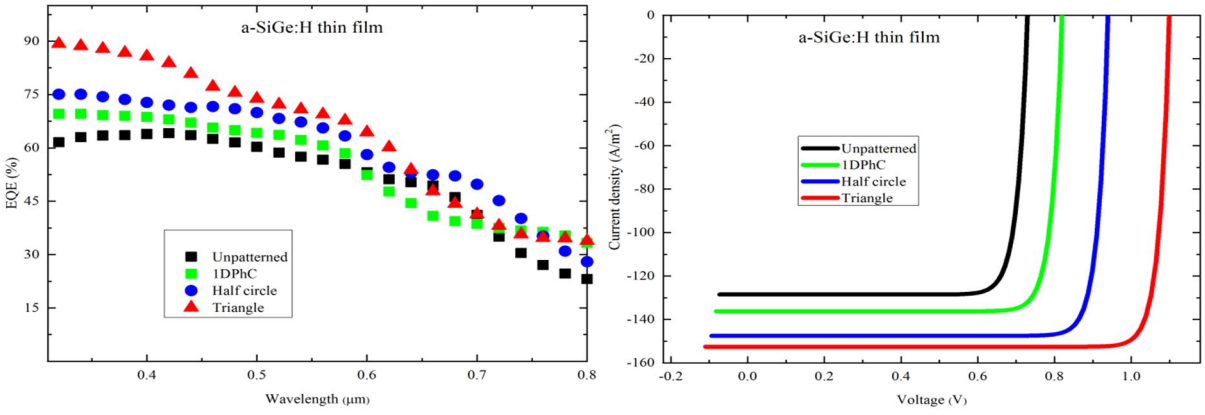

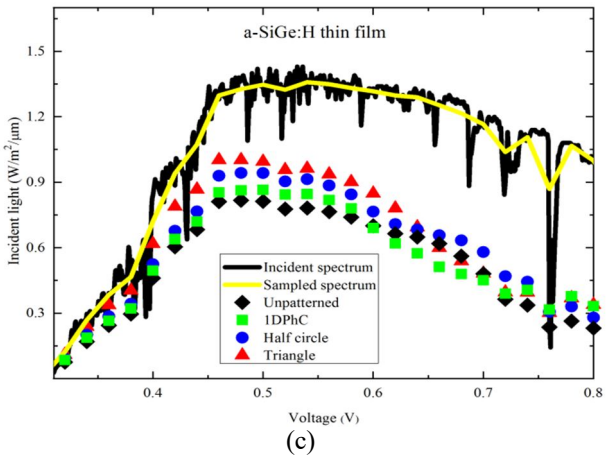

FIG. 8. (a) The EQE graphs, (b) the J-V curves and (c) the smoothened spectral distribution, studied by different grating structures studied, made by a-SiGe:H thin film.

Fig. 8.a shows the EQE graphs of a-SiGe:H thin film with diverse models of PhCs. Correspondingly, Fig. 8.b shows J-V curves of a-SiGe:H thin film solar cell with different V_{oc} and J_{sc} results values and Fig. 8.c shows the computed spectral distribution graph for the proposed simple gratings for the studied solar spectrum AM1.5. The a-SiGe:H thin film solar cell electrical output results are concise in Table 4.

TABLE 4. The energy conversion efficiency simulation results of a-SiGe:H thin film solar cell.

	Unpatterned	1DPhC	Half-circle	Triangular
P_{max}[W]	79.79	96.38	121.52	149.47
ff [%]	85.06	86.3	87.65	89.05
V_{oc}[V]	0.73	0.82	0.94	1.1
J_{sc}[A/cm^2]	128.5	136.2	147.5	152.6
J_{so}[A/cm^2]	123.6	131.6	143.1	148.7
η[%]	8.86	10.71	13.50	16.6

The a-SiGe:H thin film solar cell shows higher J_{sc} with a hydrogenated PV cell; and reducing the band gap of the absorbent layer through the growth of Germanium content within the layer is probably accompanied by V_{oc} and *ff* losses.

The better result in the a-SiGe:H semiconductor material case was in the case of triangular grating, the numerical simulation results showed that the efficiency was adequate by using a-SiGe:H with the balance of a-Si:H, owing to the presence of germanium concentration which in turn affects the use of a smaller energy band gap. The efficiency was found to reach 16.6% in the case of triangle which allows an improvement efficiency of 7.74% compared to unpatterned grating. Moreover, the triangle maximum power observed is 14.95W which makes a difference of 7.15W in comparison with the unpatterned model.

J_{sc} gradually increasing as the V_{oc} and *ff* values, as V_{oc} and *ff* remained less in the unpatterned grating thin layer than in the other grating structures especially in triangular one, which can be condoled to the loss of the improved recombination of electron hole dual in an unpatterned grating in order to the increased mean gap density [37].

The smoothened spectral distribution variation for the proposed different forgoing grating structures have shown in Fig. 8.c. Furthermore, the figure shows the performance improvement for the triangular structure as compared to the other shapes values, as shown in the previous results. Although these proposed periodic grating shapes can significantly improve the efficiency, the results achieved are still below the Lambert limits [38].

In view of decrease carrier lifetime in amorphous silicon materials, the enough carrier collection foremost rely on the inner electronic domain which play an essential function in representing and detaching the carriers for set to the electrodes, where the redistribution of Germanium atoms in absorber layer can raise V_{oc} and *ff* while this is somewhat detrimental for J_{sc} [39]. As clearly seen in Fig. 7.a and Fig. 8.a, the EQE of different structures of solar cells was decreasing gradually according to the morphological design of the studied gratings. The improvement in EQE occurs because photon beams are absorbed and then reemitted at longer emission wavelengths, where the highest value was at the beginning point of studies wavelength (0.3-0.4μm), where in triangle case reached by 0.9V; 0.72V in half circle, 0.69V in 1DPC and 0.59V was is unpatterned one. The EQE is null when the forward bias becomes less than 0.2V in all cases for the studied morphological gratings. A slighter dropping in the EQE is obvious for the bias during 0.59V and 0.9V while a comparatively considerable fall is clear for a bias over 0.9V. In triangle case, the 0.9V bias shows a very large reduction in the EQE, in this condition the carrier collection probably suffers from the high density of defects or traps which hinders their movement for the collection, can be used to distinguish the recombination losses in the forgoing thin absorber layers.

Depending on the results obtained by Yousif, B *et al*. [40], a remarkable improvement especially in a-SiGe:H semiconductor material in the triangle grating was noticed, as well as an enhancement in solar cell efficiency of 4.36%,

on other hand in the case of a-Si:H, a noticeable improvement of solar cell efficiency was estimated as 0.77%.

The electrical properties of amorphous thin film are sensitively dependent on the density of energy and the distribution of local gap states, where the main advantage of a-SiGe:H is the capacity of the unstable optical band gap to lower energies by increasing the germanium concentration in the layer [41].

The Incidence Angle (θi) Effect

In this section, the incidence angle influence of photon beams on the absorbent layer is investigated. We estimated the extent of the photon beams distribution by variation of the incidence angle from 0° to 90° in the case of a-Si:H and a-SiGe:H. Where, the incidence angle (θi) is in between a ray incident made by photon beams and the perpendicular line to the absorbent layer at the point of incidence according to Snell's law [42]:

$$\frac{\sin\theta_i}{\sin\theta_r} = \frac{n_2}{n_1} \quad (8)$$

and:

$$\theta_i = sin^{-1}\left(\frac{(\sin\theta_r \times n_2)}{n_1}\right) \quad (9)$$

where: θ_r angle of reflection; n_1 incidence medium refractive index; n_2 transmitted medium refractive index. Fig. 9 presents the changes of light absorption in absorbent layer using unpatterned, 1DPhC, half circle and triangular gratings, depending on the variation of the incidence angle from 0° to 90° with an increment of 5° in the case of both a-Si:H and a-SiGe:H.

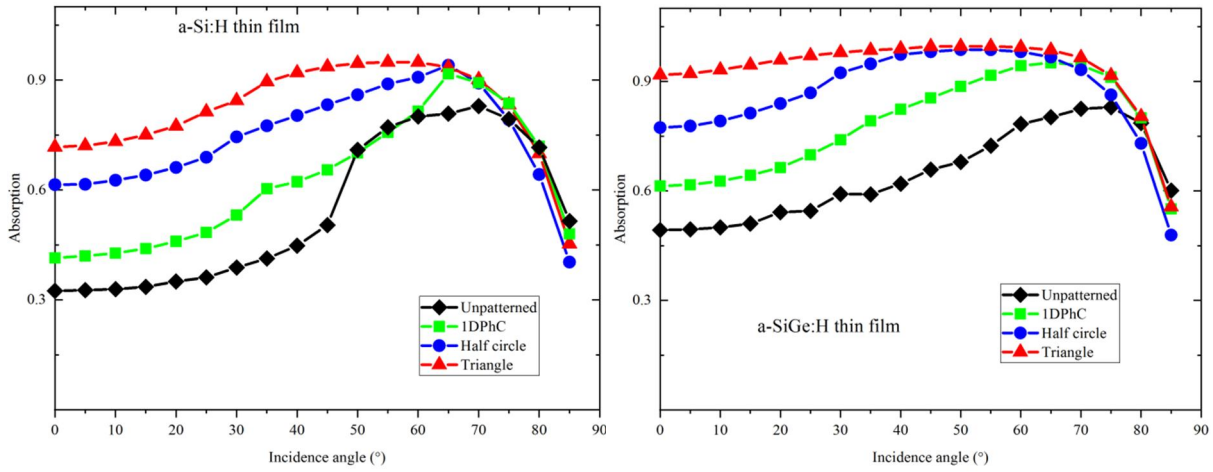

(a) (b)

FIG. 9. Incidence angle effect on absorbent layer of different gratings made by (a) a-Si:H and (b) a-SiGe:H.

The absorption ratio was increasing with increase the incidence angle until it reaches the highest absorption ratio at 50°-70°, and then it begins to decrease until it is completely absent at the horizontal position at 90°. At incident angles (50°-70°), the absorption ratio using the triangle grating improved by 14.41% compared to the unpatterned grating (Fig. 9.a and Fig. 9.b). The peak of absorption ratio is 94% in the triangle shape, 92% in the half circle, 90% in 1DPhC and it reached 79% approximately with unpatterned grating. On the other hand, in Fig. 9.b we noted the absorption ratio in a-SiGe:H is better compared with a-Si:H, while we find an enhancement in the peak (appeared in the incident angles at 50°-70°) of 5% in triangular, 4% in half-circle, 2% in 1DPhC and 2% in unpatterned gratings. Thereafter, all absorption ratios with a-Si:H and a-SiGe:H begins to decrease until they are completely absent at 90°, *i.e.*, there is no absorption (the horizontal condition: incident angle is 90°).

Correspondingly, compare with Mudachathi, R and Tanaka, T results [43], we found an enhancement in the absorption ratio, where it begins to expanded above an incident angle between 0° to 70° (maximum in the range 50° to 70°) in both a-Si:H and a-SiGe:H thin films, several studies have shown that the most appropriate angular range in which the absorption is more available is between 50° to 70°, moreover, the material quality and morphology used in addition to the climate condition with the temperature variations should be considered [44].

In addition, owing to the limited thickness of the absorbent thin film, not all photon beams are absorbed into the absorbent layer. Therefore, the absorbent layer must be thick to absorb as much light as conceivable and the thickness must not exceed the length of the carrier spread [45].

The aggregate energy engendered by the cell situated on diffraction of incident solar cell spectrum structures, is determined by materials effects, geometric dimensions, positioning, simplicity and efficient development [46]. On other hand different types of grating such as unpatterned, 1DPhC, half circle and triangle gratings play an important role in the absorption of light. Using the scattering effects enables more photon beams in the triangular shape to enter into the PV cell to enhance the absorption proficiency and the energy conversion efficiency over the other grating structures.

PV Thin film uses the back reflector to scatter photon beams, that are not absorbed through the first cell pathway. The most important function in dominating the absorption and photon beam extraction in a PV cell is joining the back reflector substrate and also redirects the unabsorbed photon beams back to the P-I-N junction which improves its retention and increases PV energy efficiency [47].

Conclusions

This work is carried out on the enhancement of the absorption of solar cells based on PhCs. Thin film absorbers were investigated based on the optical and the J-V characteristics.

The performances delivered by the cells depend critically on the morphology and the material type of the absorbent thin film, in particular to involve the quality of absorption in thin film cells.

The RCWA method is the one used in this work. The different properties of unpatterned materials were studied as well as the properties of 1DPhC, half circle, and triangular lattice structures for two types of materials namely; a-Si:H and a-SiGe:H. The study showed that the latter is more efficient.

The incidence angle effect on both materials was also studied. The results showed that the significant improvement in optical and electrical characteristics occurs for the triangular grating especially in the a-SiGe:H case with an enhancement of 16.6% solar cell efficiency in the case of triangle which allows an improvement efficiency of 7.74% compared to unpatterned grating. Moreover, the triangle maximum power observed is 14.95W which makes a difference of 7.15W in comparison with the unpatterned model, and in an ideal incidence angle between 50° and 70°.

The a-SiGe:H is found to be more efficient in terms of the optical and electrical properties for PV applications.

Acknowledgment

The authors would like to acknowledge the financial support for this work by grants from General Direction of Scientific Research and Technological Development (GDSRTD) at the Ministry of Higher Education and Scientific Research of Algeria.

References

[1] Chhajed, S., Schubert, M.F., Kim, J.K. and Schubert, E.F., Appl. Phys. Lett., 93 (2008) 251108.

[2] Choubey, P.C., Oudhia, A. and Dewangan, R., RRST., 4 (8) (2012).

[3] Solanki, C.S. and Singh, H.K, "Anti-reflection and Light Trapping in c-Si Solar Cells", Edn. C.S. Solanki and H.K. Singh, (Springer, Singapore, 2017) pp. 1-16.

[4] Liu, W., Ma, H. and Walsh, A., Renewable and Sustainable Energy Reviews, 116 (2019) 109436.

[5] Kedia, S. and Vijaya, R., Bull. Mater. Sci., 34 (2) (2011) 383.

[6] Stoumpos, C.C. and Kanatzidis, M.G., Advanced Materials, 28 (28) (2016) 5778.

[7] Green, M.A., Hishikawa, Y., Dunlop, E.D., Levi, D.H., Hohl-Ebinger, J. and Ho-Baillie, A.W., Progress in Photovoltaics: Research and Applications, 26 (7) (2018) 427.

[8] Smith, D.D., Reich, G., Baldrias, M., Reich, M., Boitnott, N. and Bunea, G., Proc. Intern. Conf. on IEEE 43rd Photovoltaic Specialists, Portland, USA, (2016), pp. 3351.

[9] Yoshikawa, K., Kawasaki, H., Yoshida, W., Irie, T., Konishi, K., Nakano, K., Uto, T., Adachi, D., Kanematsu, M., Uzu, H. and Yamamoto, K., Nature Energy, 2 (5) (2017) 1.

[10] Green, M.A., Dunlop, E.D., Hohl-Ebinger, J., Yoshita, M., Kopidakis, N.and Ho-Baillie, A.W., Progress in Photovoltaics: Research and Applications, 28 (1) (2020) 3.

[11] Kirchartz, T. and Rau, U., Advanced Energy Materials, 8 (28) (2018) 1703385.

[12] Dobson, D.C., Journal of Computational Physics, 149 (2) (1999) 363.

[13] Zeng, L., Yi, Y., Hong, C., Liu, J., Feng, N., Duan, X., Kimerling, L.C. and Alamariu, B.A., Appl. Phys. Lett., 89 (11) (2006) 111111.

[14] Xu, X., Yang, J. and Guha, S., Journal of Non-crystalline Solids, 198 (1996) 60.

[15] Si, F.T., Isabella, O. and Zeman, M., Solar Energy Materials and Solar Cells, 163 (2017) 9.

[16] RSoft Design Group, DiffractMOD, Executive Blvd, Inc. 200 (2013) 10562.

[17] Reiss, H., Fuller, C.S. and Morin, F.J., Bell System Technical Journal, 35 (3) (1956) 535.

[18] Shima, M., Isomura, M., Wakisaka, K.I., Murata, K. and Tanaka, M., Solar energy Materials and Solar Cells, 85 (2) (2005) 167.

[19] Veldhuizen, L.W., Vijselaar, W.J., Gatz, H.A., Huskens, J. and Schropp, R.E., Thin Solid Films, 635 (2017) 66.

[20] Schropp, R.E., Carius, R. and Beaucarne, G., MRS Bulletin, 32 (3) (2007) 219.

[21] Huang, Y.C., Chan, C.C., Kuan, S.C., Wang, S.J. and Lee, S.K., International Journal of Photoenergy, 2014 (2014) 615860.

[22] Idda, A., Ayat, L. and Dahbi, N., Journal of Ovonic Research, 15 (5) (2019).

[23] Hench, J.J. and Strakos, Z.D.E.N.E.K., Electronic Transactions on Numerical Analysis, 31 (2008) 331.

[24] Li, L., J. Opt. Soc. Am. A, 14 (10) (1997) 2758.

[25] Popov, E. and Nevière, M., J. Opt. Soc. Am. A, 18 (11) (2001) 2886.

[26] Ouanoughi, A., Hocini, A. and Khedrouche, D., Front. Optoelectron, 9 (1) (2016) 93.

[27] Wang, L., Zheng, Z., Gou, Y., Liang, W. and Yu, W., Optics Communications, 483 (2021) 126673.

[28] Nam, Y.M., Huh, J. and Jo, W.H., Solar Energy Materials and Solar Cells, 94 (6) (2010) 1118.

[29] Dominguez, S., Garcia, O., Ezquer, M., Rodriguez, M.J., Lagunas, A.R., Pérez-Conde, J. and Bravo, J., Photonics and Nanostructures-Fundamentals and Applications, 10 (1) (2012) 46.

[30] Heidarzadeh, H. and Tavousi, A., Materials Science and Engineering: B, 240 (2019) 1.

[31] Che, X., Li, Y., Qu, Y. and Forrest, S.R., Nature Energy, 3 (5) (2018) 422.

[32] Raiford, J.A., Belisle, R.A., Bush, K.A., Prasanna, R., Palmstrom, A.F., McGehee, M.D. and Bent, S.F., Sustainable Energy & Fuels, 3 (6) (2019) 1517.

[33] Wu, W. and Magnusson, R., Opt. Lett., 37 (11) (2012) 2103.

[34] Taguchi, M., Terakawa, A., Maruyama, E. and Tanaka, M., Progress in Photovoltaics: Research and Applications,13 (6) (2005) 481.

[35] Schuttauf, J.W., Niesen, B., Lofgren, L., Bonnet-Eymard, M., Stuckelberger, M., Hanni, S., Boccard, M., Bugnon, G., Despeisse, M., Haug, F.J, Meillaud, F. and Ballif, C., Solar Energy Materials and Solar Cells, 133 (2015) 163.

[36] Qi, B. and Wang, J., Phys. Chem. Chem. Phys., 15 (23) (2013) 8972.

[37] Moon, S.Y., You, D.J., Lee, S.E. and Lee, H., Current Applied Physics, 13 (7) (2013) 1502.

[38] Gupta, N.D. and Janyani, V., IEEE J. Quantum Electron., 53 (2) (2017) 1.

[39] Chung, J.W., Park, J.W., Lee, Y.J., Ahn, S.W., Lee, H.M. and Park, O.O., Jpn. J. Appl. Phys., 51 (10S) (2012) 10NB16.

[40] Yousif, B., Abo-Elsoud, M.E.A. and Marouf, H., Optical and Quantum Electronics, 51 (8) (2019) 1.

[41] Gordijn, A., Zambrano, R.J., Rath, J.K. and Schropp, R.E., IEEE Transactions on Electron Devices, 49 (5) (2002) 949.

[42] Stigloher, J., Decker, M., Körner, H.S., Tanabe, K., Moriyama, T., Taniguchi, T., Hata, H., Madami, M., Gubbiotti, G., Kobayashi, K., Ono, T. and Back, C.H., Phys. Rev. Lett., 117 (3) (2016) 037204.

[43] Mudachathi, R. and Tanaka, T., Adv. Nat. Sci: Nanosci. Nanotechnol., 9 (1) (2018) 015010.

[44] Al Garni, H.Z., Awasthi, A. and Wright, D., Renewable Energy, 133 (2019) 538.

[45] Sane, M., Sahin, G., Barro, F.I. and Maiga, A.S., Turk. J. Phys., 38 (2) (2014) 221.

[46] Sadoun, B., Mouetsi, S., Hocini, A. and Hocini, A., IOP Conf. Ser.: Mater. Sci. Eng., 1046 (1) (2021) 012014.

[47] Bhattacharya, S. and John, S., APL Photonics, 5 (2) (2020) 020902.